

# The full curvature effect expected in early X-ray afterglow emission of gamma-ray bursts

Y.-P. Qin<sup>1,2</sup>

## ABSTRACT

We explore the influence of the full curvature effect on the flux of early X-ray afterglow of gamma-ray bursts (GRBs) in cases when the spectrum of the intrinsic emission is a power-law. We find that the well-known  $t^{-(2+\beta)}$  curve is present only when the intrinsic emission is extremely short or the emission arises from an exponential cooling. The time scale of this curve is independent of the Lorentz factor. The resulting light curve would contain two phases when the intrinsic emission has a power-law spectrum and a temporal power-law profile with infinite duration. The first phase is a rapid decay one where the light curve well follows the  $t^{-(2+\beta)}$  curve. The second is a shallow decay phase where the power-law index of the light curve is obviously smaller than that in the first phase. The start of the shallow phase is strictly constrained by the fireball radius, which in turn, can put a lower limit to the latter. In the case when the temporal power-law emission lasts a limited interval of time, there will be a third phase after the  $t^{-(2+\beta)}$  curve and the shallow decay phase, which is much steeper than the shallow phase. As an example of application, we fit the XRT data of GRB 050219A with our model and show that the curvature effect alone can roughly account for this burst. Although fitting parameters can not be uniquely determined due to various choices of fitting, a lower limit of the fireball radius of this burst can be estimated, which is  $\sim 10^{14}cm$ .

*Subject headings:* gamma-rays: bursts — gamma-rays: theory — relativity

## 1. Introduction

The canonical X-ray afterglow light curve containing five components after the prompt emission phase is a great finding of Swift (Chincarini et al. 2005; Nousek et al. 2006; O’Brien

---

<sup>1</sup>Center for Astrophysics, Guangzhou University, Guangzhou 510006, P. R. China; ypqin@gzhu.edu.cn

<sup>2</sup>Physics Department, Guangxi University, Nanning 530004, P. R. China

et al. 2006; Zhang et al. 2006; Zhang 2007). The first of the five is the so-called “steep decay phase” which generally extends to  $\sim (10^2 - 10^3)s$ , with a temporal decay slope typically  $-3$  or much steeper (Vaughan et al. 2006; Cusumano et al. 2006; O’Brien et al. 2006).

A hint in this phase suggesting the emission of high latitude fireball surface is that it is typically smoothly connected to the prompt emission phase (Tagliaferri et al. 2005; Barthelmy et al. 2005; Liang et al. 2006). Generally, the steep decay phase was interpreted as a consequence of the so-called curvature effect (Fenimore et al. 1996; Kumar & Panaitescu 2000; Dermer 2004; Dyks et al. 2005; Butler & Kocevski 2007a; Liang et al. 2006; Panaitescu et al. 2006; Zhang et al. 2006; Zhang et al. 2007). The curvature effect is a combined effect that includes the delay of time and the shifting of the intrinsic spectrum as well as other relevant factors of an expanding fireball (see Qin et al. 2006 for a detailed explanation). The effect was intensively studied recently in the prompt gamma-ray phase, where the profile of the full light curve of pulses, the spectral lags, the power-law relation between the pulse width and energy, and the evolution of the hardness ratio curve are concerned (Sari & Piran 1997; Qin 2002; Ryde & Petrosian 2002; Kocevski et al. 2003; Qin & Lu 2005; Shen et al. 2005; Lu et al. 2006; Peng et al. 2006; Qin et al. 2004, 2005, 2006).

As early as a decade ago, Fenimore et al. (1996) found that, due to the curvature effect, light curves arising from the emission of an infinitely thin shell would be a power-law of observational time when the rest-frame photon number spectrum is a power-law and the emission is within an infinitesimal time interval. In this case, the two power-law indexes are related by  $\alpha = 2 + \beta$ , where  $\alpha$  is the light curve index and  $\beta$  the spectral index. In concerning the X-ray afterglow emission, Kumar & Panaitescu (2000) also found that, due to the curvature effect, the light curve of a shocked heated fireball shell radiating with a power-law spectrum within the observational band (i.e., the X-ray band in the early afterglow observation) is a power-law of time as well and relation  $\alpha = 2 + \beta$  holds in this situation.

As revealed in Fig. 7 of Nousek et al. (2006), relation  $\alpha = 2 + \beta$  is roughly in agreement with the data in the steep decay phase of some Swift bursts. However, the figure also shows that real relations between the two indexes of some bursts significantly deviate from the  $\alpha = 2 + \beta$  curve. This might be due to the ill re-setting of time that should be set to the real time when the central engine restarts (see Liang et al. 2006). In addition, more or less subtracting the underlying afterglow contribution would lead to other values of the temporal index  $\alpha$  (for a detailed explanation, see Zhang 2007).

We notice that the derivation of relation  $\alpha = 2 + \beta$  in previous papers is based on the main part of the curvature effect. Does it still hold (or, in what situation it would still hold) when the full curvature effect is considered? This motivates our investigation below. The structure of the paper is as follows. In Section 2, we present a general analysis on the full

curvature effect in cases when the intrinsic emission is a power-law. In Section 3, we discuss light curves of power-law emission associated with several typical intrinsic temporal profiles. Presented in Section 4 is an example of application of our model. Conclusions are presented in the last section.

## 2. Light curves of fireballs arising from the intrinsic emission with a power-law spectrum

Observation of the emission arising from an expanding fireball would be influenced by the delay of time of different areas of the fireball surface, the variation of the intensity due to the growing of the fireball radius, the variation of the time contracted factor and the shifting of the intrinsic spectrum associated with the angle to the line of sight. Taking all these factors into account, one comes to a full knowledge of the so-called curvature effect (see also Qin et al. 2006 for a detailed explanation). Consider a constant expanding fireball shell emitting within proper time interval  $t_{0,\min} \leq t_0 \leq t_{0,\max}$  and over the fireball area confined by  $\theta_{\min} \leq \theta \leq \theta_{\max}$ , where  $\theta$  is the angle to the line sight. Assume that the energy range of the emission is not limited. Following the same approach adopted in Qin (2002) and Qin et al. (2004), one can verify that the flux tensity expected by a distant observer measured at laboratory time  $t_{ob}$  is

$$f_\nu(t_{ob}) = \frac{2\pi c^2 \int_{\tilde{t}_{0,\min}}^{\tilde{t}_{0,\max}} I_{0,\nu}(t_0, \nu_0) [(t_0 - t_{0,c})\Gamma + D/c - (t_{ob} - t_c)][R_c/c + (t_0 - t_{0,c})\Gamma(v/c)]^2 dt_0}{D^2 \Gamma^2 \{R_c/c - [D/c - (t_{ob} - t_c)](v/c)\}^2}, \quad (1)$$

where  $\tilde{t}_{0,\min}$  and  $\tilde{t}_{0,\max}$  are determined by

$$\tilde{t}_{0,\min} = \max\left\{t_{0,\min}, \frac{t_{ob} - t_c - D/c + (R_c/c) \cos \theta_{\max}}{[1 - (v/c) \cos \theta_{\max}]\Gamma} + t_{0,c}\right\} \quad (2)$$

and

$$\tilde{t}_{0,\max} = \min\left\{t_{0,\max}, \frac{t_{ob} - t_c - D/c + (R_c/c) \cos \theta_{\min}}{[1 - (v/c) \cos \theta_{\min}]\Gamma} + t_{0,c}\right\}, \quad (3)$$

respectively, and  $\nu_0$  and  $t_0$  are related by

$$\nu_0 = \frac{R_c/c - [D/c - (t_{ob} - t_c)](v/c)}{R_c/c + (t_0 - t_{0,c})\Gamma} \Gamma \nu. \quad (4)$$

The observation time is confined by

$$\begin{aligned} & [1 - (v/c) \cos \theta_{\min}][(t_{0,\min} - t_{0,c})\Gamma + t_c] + [t_c(v/c) - R_c/c] \cos \theta_{\min} + D/c \leq t_{ob} \\ & \leq [1 - (v/c) \cos \theta_{\max}][(t_{0,\max} - t_{0,c})\Gamma + t_c] + [t_c(v/c) - R_c/c] \cos \theta_{\max} + D/c \end{aligned} \quad (5)$$

Beyond this time interval, no photons of the emission are detectable by the observer.

A power-law spectrum was commonly observed in early X-ray afterglow especially in the steep decay phase (e.g., Vaughan et al. 2006; Cusumano et al. 2006; O’Brien et al. 2006). In this paper we focus our attention only on the case of the intrinsic emission with a power-law spectrum which is expectable in the case of synchrotron emission produced by shocks and was generally assumed in previous investigations (e.g., Fenimore et al. 1996; Sari et al. 1998; Kumar & Panaitescu 2000). Let the intensity of the intrinsic emission be  $I_{0,\nu}(t_0, \nu_0) = I_0(t_0)\nu_0^{-\beta}$  (Kumar and Panaitescu 2000). One gets from equation (1) that

$$f_\nu(t_{ob}) = \frac{2\pi c^2 \nu^{-\beta} \int_{\tilde{t}_{0,\min}}^{\tilde{t}_{0,\max}} I_0(t_0) [R_c/c + (t_0 - t_{0,c})\Gamma v/c]^{2+\beta} [(t_0 - t_{0,c})\Gamma + D/c - (t_{ob} - t_c)] dt_0}{D^2 (\Gamma v/c)^{2+\beta} (t_{ob} - t_c + R_c/v - D/c)^{2+\beta}}, \quad (6)$$

where relation (4) is applied. Assigning

$$t \equiv t_{ob} - t_c + R_c/v - D/c, \quad (7)$$

one comes to

$$f_\nu(t) = \frac{2\pi c^2 \nu^{-\beta}}{D^2 (\Gamma v/c)^{2+\beta} t^{2+\beta}} \int_{\tilde{t}_{0,\min}}^{\tilde{t}_{0,\max}} I_0(t_0) [R_c/c + (t_0 - t_{0,c})\Gamma v/c]^{2+\beta} [(t_0 - t_{0,c})\Gamma + R_c/v - t] dt_0, \quad (8)$$

with

$$\tilde{t}_{0,\min} = \max\left\{t_{0,\min}, \frac{t - R_c/v + (R_c/c) \cos \theta_{\max}}{[1 - (v/c) \cos \theta_{\max}]\Gamma} + t_{0,c}\right\}, \quad (9)$$

$$\tilde{t}_{0,\max} = \min\left\{t_{0,\max}, \frac{t - R_c/v + (R_c/c) \cos \theta_{\min}}{[1 - (v/c) \cos \theta_{\min}]\Gamma} + t_{0,c}\right\}, \quad (10)$$

$$\nu_0 = \frac{t}{R_c/v + (t_0 - t_{0,c})\Gamma} \Gamma \nu, \quad (11)$$

and

$$\begin{aligned} & [1 - (v/c) \cos \theta_{\min}] [(t_{0,\min} - t_{0,c})\Gamma + t_c] + [t_c(v/c) - R_c/c] \cos \theta_{\min} + R_c/v - t_c \leq t \\ & \leq [1 - (v/c) \cos \theta_{\max}] [(t_{0,\max} - t_{0,c})\Gamma + t_c] + [t_c(v/c) - R_c/c] \cos \theta_{\max} + R_c/v - t_c \end{aligned} \quad (12)$$

The meaning of  $t$  defined by equation (7) can be revealed by employing equation (8) in Qin et al. (2004) (where quantity  $t$  is now written as  $t_{ob}$ ). According to equation (8) in Qin et al. (2004), emission from  $R_c = 0$  (this emission occurs at  $t_\theta = t_c$ ) corresponds to  $t = 0$ ; and emission from the area of  $\theta = 0$  from any  $R_c$  (occurring at  $t_\theta = t_c$ ) gives rise to  $t = (R_c/v)(1 - \beta) \simeq (R_c/v)/2\Gamma^2$ . Quantity  $(R_c/v)/2\Gamma^2$  is nothing but the traveling time of the fireball surface from the explosion spot to  $R_c$ , contracted by factor  $1/2\Gamma^2$  since the area

of  $\theta = 0$  moves towards the observer with Lorentz factor  $\Gamma$ . Thus,  $t = 0$  is the moment when photons emitted from  $R_c = 0$  reach the observer. Even for  $t_\theta = t_c$ , one would have  $t > 0$  if  $R_c > 0$ . The emission time  $t_\theta = t_c$  does not mean that photons are radiated at  $R_c = 0$ . In stead, it means that these photons are emitted from the surface of the fireball with radius  $R_c$  which is measured at  $t_c$  (see Qin 2002 Appendix A).

Note that when the power-law range is limited, then it would constrain the integral limits  $\tilde{t}_{0,\min}$  and  $\tilde{t}_{0,\max}$  which are different from equations (2) and (3), or (9) and (10) (see Qin 2002). In the following, we adopt the Kumar & Panaitescu (2000)'s assumption: the intrinsic emission is a strict power-law within the energy range corresponding to the observed energy channel. Thus, equations (2) and (3), or (9) and (10) are applicable.

According to (9) and (10),  $\int_{\tilde{t}_{0,\min}}^{\tilde{t}_{0,\max}} I_0(t_0)[R_c/c + (t_0 - t_{0,c})\Gamma v/c]^{2+\beta} [(t_0 - t_{0,c})\Gamma + R_c/v - t] dt_0$  is only a function of  $t$ . Let

$$h(t) \equiv \int_{\tilde{t}_{0,\min}}^{\tilde{t}_{0,\max}} I_0(t_0)[R_c/c + (t_0 - t_{0,c})\Gamma v/c]^{2+\beta} [(t_0 - t_{0,c})\Gamma + R_c/v - t] dt_0. \quad (13)$$

Equation (8) could then be written as

$$f_\nu(t) = \frac{2\pi c^2}{D^2(\Gamma v/c)^{2+\beta}} h(t) t^{-(2+\beta)} \nu^{-\beta}. \quad (14)$$

It shows that, in the case that the power-law intrinsic radiation intensity  $I_{0,\nu}(t_0, \nu_0) = I_0(t_0)\nu_0^{-\beta}$  holds within the energy range which corresponds to the observed energy channel due to the Doppler shifting, a power-law spectrum will also hold within the observed channel and the index will be exactly the same as that in the intrinsic spectrum.

Taking factor  $h(t)$  as a constant, equation (14) gives rise to

$$f_\nu(t) \propto t^{-(2+\beta)} \nu^{-\beta}. \quad (15)$$

This is the well-known flux density associated with the curvature effect, which reveals the relation between the temporal and spectral power-law indexes:  $\alpha = 2 + \beta$ , where  $\alpha$  is the temporal index (e.g., when assuming  $f_\nu(t) \propto t^{-\alpha}$ ) (see Fenimore et al. 1996; Kumar & Panaitescu 2000).

### 3. Time factors other than the power-law function

Let us consider an intrinsic emission with a  $\delta$  function of time. In this situation, effects arising from the duration of real intrinsic emission will be omitted and therefore those merely coming from the expanding motion of the fireball surface will be clearly seen.

Not losing generality, we assume that  $I_0(t_0) = I_0\delta(t_0 - t_{0,c})$  and take  $\theta_{\min} = 0$  and  $\theta_{\max} = \pi/2$  (this corresponds to the half fireball surface facing us, which will be taken throughout this paper). One then gets from (12) that

$$R_c/v - R_c/c \leq t \leq R_c/v. \quad (16)$$

Within the observation time confined by (16), the integral (13) becomes

$$h(t) = I_0(R_c/c)^{2+\beta}(R_c/v - t). \quad (17)$$

Therefore,

$$f_\nu(t) = \frac{2\pi c^2 I_0 (R_c/\Gamma v)^{2+\beta}}{D^2} (R_c/v - t) t^{-(2+\beta)} \nu^{-\beta}. \quad (18)$$

When  $t$  is beyond the time range confined by (16),  $h(t) = 0$  and then  $f_\nu(t) = 0$ .

Based on Qin (2002) and Qin et al. (2004), one can check that the term  $[(t_0 - t_{0,c})\Gamma + D/c - (t_{ob} - t_c)]$  in equation (1), or the term  $[(t_0 - t_{0,c})\Gamma + R_c/v - t]$  in equation (13), comes from the projected factor of the infinitesimal fireball surface area in the angle concerned (say,  $\theta$ ) to the distant observer, which is known as  $\cos\theta$ . This term becomes  $R_c/v - t$  for a  $\delta$ -function temporal radiation when adopting the new time definition (7). Corresponding to larger observation times, the line of sight angles of the emitted areas are larger, and then the term  $\cos\theta$  becomes smaller.

Note that when one considers only a very small cone towards the observer, this term could be ignored since it varies very mildly within the angle range close to  $\theta = 0$ . However, what we discuss here is the steep decay phase of early X-ray afterglow which was generally assumed to arise from high latitude emission. In this situation, the variation of this term would be significant.

According to (11), another noticeable term,  $[R_c/c + (t_0 - t_{0,c})\Gamma v/c]$ , in equation (1) or (13) reflects the shifting of frequency. Equation (11) suggests that the flux observed at frequency  $\nu$  and time  $t$  will be contributed by rest-frame photons of frequency  $\nu_0$  emitted at proper time  $t_0$  (note that the flux will also be contributed by rest-frame photons of other frequency  $\nu'_0$  emitted at other proper time  $t'_0$  so long as they satisfy equation (11), and the value of the flux is determined by all these possible photons). Quantity  $[R_c/c + (t_0 - t_{0,c})\Gamma v/c]$  is a shifting factor of the frequency when observation time  $t$  is fixed. This term is independent of observation time, but due to its coupling with  $(t_0 - t_{0,c})\Gamma$  in the term of  $[(t_0 - t_{0,c})\Gamma + D/c - (t_{ob} - t_c)]$ , it might also affect the light curve.

Similarly, the term  $I_0(t_0)$  might also play a role due to its coupling with  $(t_0 - t_{0,c})\Gamma$  in the term  $[(t_0 - t_{0,c})\Gamma + D/c - (t_{ob} - t_c)]$ .

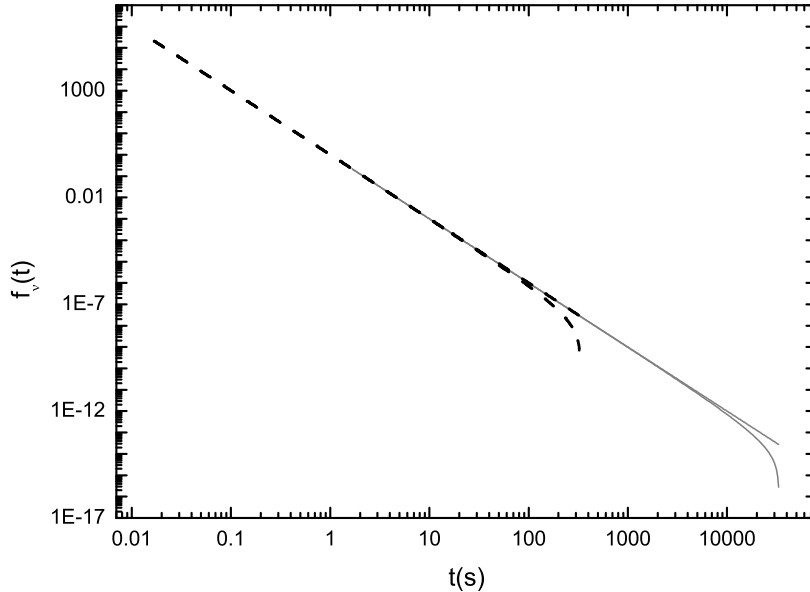


Fig. 1.— Light curves  $I_{\nu,\delta}[1 - t/(R_c/v)]t^{-(2+\beta)}$  (lower lines) and  $I_{\nu,\delta}t^{-(2+\beta)}$  (upper lines) associated with  $R_c \simeq 10^{15}cm$  (solid lines) and  $R_c \simeq 10^{13}cm$  (dashed lines). Note that the lower and upper lines are overlapped in the main domain of the corresponding light curves.

The last factor affecting the profile of light curves is the integral range of equation (13). The integral range might differ from time to time since the fireball surface area that sends photons to the observer, which are observed at time  $t$ , might change with time. Shown in (9) and (10), both  $\tilde{t}_{0,\min}$  and  $\tilde{t}_{0,\max}$  are determined by observation time  $t$ . A time dependent integral range in equation (13) probably could make the decay phase of the light curve deviate from a strict power-law one.

In the following, we show how these time factors affect the decay phase of light curves which arise from the intrinsic emission with a power-law spectrum.

### 3.1. In the case of the temporal profile of the intrinsic emission being a $\delta$ -function of time

We first consider the case of the temporal profile of the intrinsic emission being a  $\delta$ -function of time. The light curve arising from this emission is  $I_{\nu,\delta}[1 - t/(R_c/v)]t^{-(2+\beta)}$  according to (18). We take  $I_{\nu,\delta} = 1$  and  $\beta = 1$  to plot the curves. We consider the fireball radius with  $R_c/v = (1/3)10^5s$  and  $R_c/v = (1/3)10^3s$  which correspond to two typical radius  $R_c \simeq 10^{15}cm$  and  $R_c \simeq 10^{13}cm$  respectively (see Ryde & Petrosian 2002).

Shown in Fig. 1 are the light curves of  $I_{\nu,\delta}[1 - t/(R_c/v)]t^{-(2+\beta)}$  and  $I_{\nu,\delta}t^{-(2+\beta)}$  associated with  $R_c \simeq 10^{15}cm$  and  $R_c \simeq 10^{13}cm$ . We find that, in the case of very short intrinsic emission, although the  $R_c/v - t$  term in equation (18) plays a role in the decay phase, the temporal curve well follow a power-law in the main domain of the phase. Following the power-law curve is a tail falling off speedily due to the effect of the  $R_c/v - t$  term. A remarkable feature revealed by the figure is that the power-law decay time is solely determined by and very sensitive to the radius of the fireball and the power-law range itself can tell how large is a fireball radius. For example, a power-law range being found to extend to 100s must be larger than  $10^{13}cm$  and that being found to extend to 10000s must be larger than  $10^{15}cm$ . The conclusion is surprisingly to be independent of the Lorentz factor. Note that this conclusion holds when the intrinsic emission is extremely short so that its temporal profile can be treated as a  $\delta$ -function. As illustrated in Fig. 1, a strict  $t^{-(2+\beta)}$  curve followed by a speedily falling off tail is a feature of extremely short intrinsic emission. When this feature is observed, one can estimate the fireball radius merely from the time scale of the power-law decay phase so long as the spectrum is a power-law and the relation of  $\alpha = 2 + \beta$  holds.

### 3.2. In the case of the temporal profile of the intrinsic emission being an exponential function of time

Second, let us consider the intrinsic emission with its temporal profile being an exponential of time and check if the resulting light curve is different from that arising from the  $\delta$ -function emission. We ignore the contribution from the rise phase of the emission of shocks (it corresponds to the situation when the rise time is extremely short). The intrinsic decaying light curve with an exponential form is assumed to be:  $I_0(t_0) = I_0 \exp[-(t_0 - t_{0,c})/\sigma_d]$  for  $t_0 > t_{0,c}$ . Equation (14) now becomes

$$f_\nu(t) = I_e h_e(t) t^{-(2+\beta)} \nu^{-\beta}, \quad (19)$$



with

$$h_e(t) = \int_{\tilde{t}_{0,\min}}^{\tilde{t}_{0,\max}} \frac{[1 + (t_0 - t_{0,c})\Gamma v/R_c]^{2+\beta} [(t_0 - t_{0,c})\Gamma v/R_c + 1 - tv/R_c] dt_0}{\exp[(t_0 - t_{0,c})/\sigma_d]} \quad (t_0 > t_{0,c}), \quad (20)$$

$$\tilde{t}_{0,\min} = \max\left\{t_{0,c}, \frac{t - R_c/v}{\Gamma} + t_{0,c}\right\} \quad (21)$$

and

$$\tilde{t}_{0,\max} = \frac{t - R_c/v + R_c/c}{(1 - v/c)\Gamma} + t_{0,c}, \quad (22)$$

where  $I_e$  is a constant and observation time  $t$  is confined by

$$R_c/v - R_c/c \leq t. \quad (23)$$

Not losing generality, we take  $t_{0,c} = 0$ . Equations (20)-(22) then become

$$h_e(t) = \int_{\tilde{t}_{0,\min}}^{\tilde{t}_{0,\max}} \frac{(1 + t_0\Gamma v/R_c)^{2+\beta} (t_0\Gamma v/R_c + 1 - tv/R_c) dt_0}{\exp(t_0/\sigma_d)} \quad (t_0 > 0), \quad (24)$$

$$\tilde{t}_{0,\min} = \max\left\{0, \frac{t - R_c/v}{\Gamma}\right\} \quad (25)$$

and

$$\tilde{t}_{0,\max} = \frac{t - R_c/v + R_c/c}{(1 - v/c)\Gamma}. \quad (26)$$

Here, we take  $I_e = 1$ ,  $\beta = 1$ , and adopt  $R_c/v = (1/3)10^5 s$  to plot the light curves. For the Lorentz factor, we take  $\Gamma = 10$  and  $\Gamma = 100$ , respectively.

Shown in Fig. 2 are the light curves plotted with different values of the width of the exponential function ( $\sigma_d = 0.1s, 1s, 10s$  and  $100s$ ). The light curves are quite similar to those arising from the intrinsic emission with its temporal profile being a  $\delta$ -function of time (see Fig. 1, where a feature of a  $t^{-(2+\beta)}$  curve followed by a speedily falling off tail is observed). Due to the contribution of the exponential decay curve of the intrinsic emission, the range of light curves is slightly larger than that in the case of the intrinsic emission with a  $\delta$ -function of time (this can be observed when the width is large enough; see the lower right panel of Fig. 2). This is understandable since after the width the emission of an exponential function dies away rapidly and therefore its contribution can be ignored.

In the case when both the width of the exponential function emission and the Lorentz factor of the fireball are large, the resulting light curve would obviously deviate from that arising from the  $\delta$ -function emission in the domain of the falling off tail, where the slope of the tail of the former light curve becomes obviously mild (see the lower right panel of Fig. 2). Besides this, no other characteristics can distinguish the tow kinds of light curve.

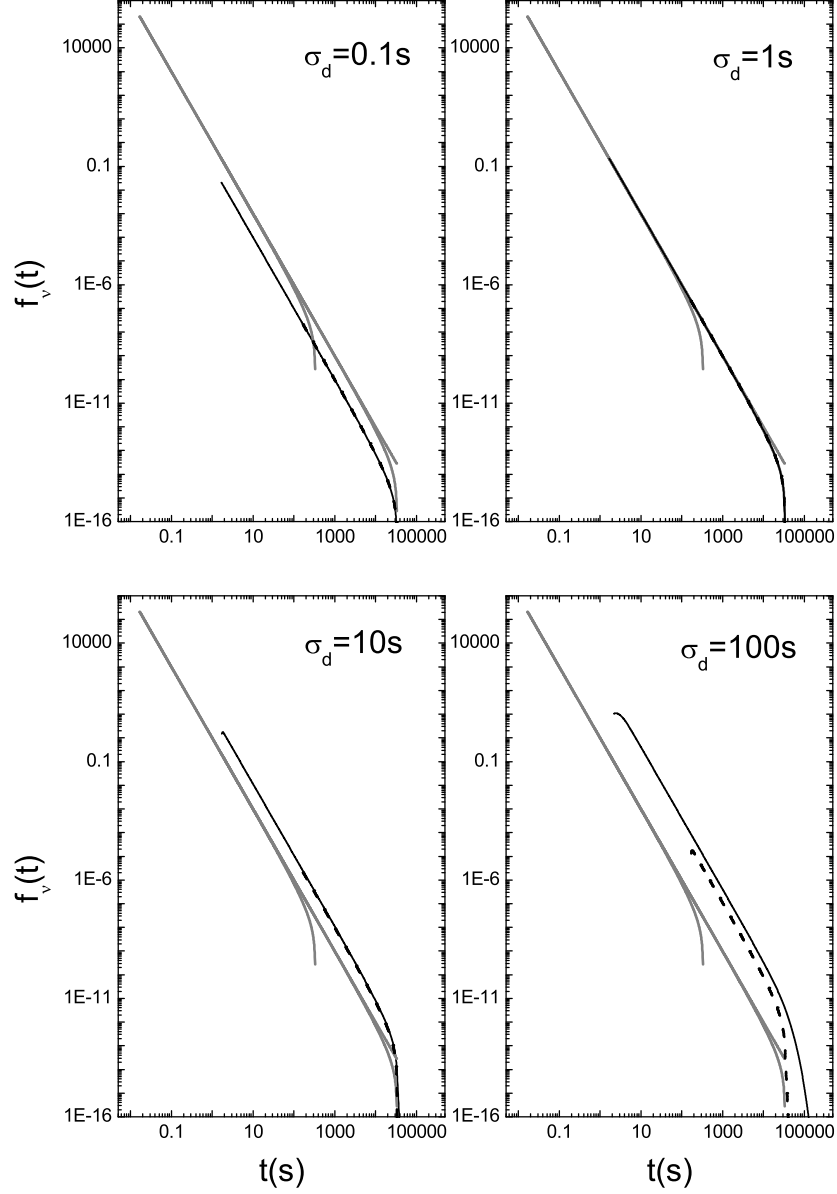


Fig. 2.— Light curves (solid lines for  $\Gamma = 100$ ; dashed lines for  $\Gamma = 10$ ) arising from the intrinsic emission with its temporal profile being an exponential function of time (see equation (19)), plotted in cases of  $\sigma_d = 0.1s$ ,  $1s$ ,  $10s$  and  $100s$  respectively, where  $h_e(t)$  is determined by (24). For the sake of comparison, those lines in Fig. 1 are also plotted (the grey color lines).

### 3.3. In the case of the temporal profile of the intrinsic emission being a power-law function of time

Third, we check if an observed light curve arising from the emission with a power-law spectrum has something to do with the intrinsic decaying behavior when the decay curve is a power-law of time. Here, we also ignore the contribution from the rise phase of the emission of shocks, and then consider only an intrinsic power-law decay emission (this will occur when the cooling is a power law).

#### 3.3.1. When the power-law decay time is infinity

Assuming that the power-law decay time is infinity, the intrinsic decaying light curve is taken as  $I_0(t_0) = [(t_0 - t_{0,c})/(t_{0,0} - t_{0,c})]^{-\alpha_0}$  for  $t_0 > t_{0,0}$ , where  $t_{0,0} > t_{0,c}$  is a constant which is the time when the power-law decay emission begins. In this case, equation (14) becomes

$$f_\nu(t) = I_p h_p(t) t^{-(2+\beta)} \nu^{-\beta}, \quad (27)$$

with

$$h_p(t) = \int_{\tilde{t}_{0,\min}}^{\tilde{t}_{0,\max}} \frac{[1 + (t_0 - t_{0,c})\Gamma v/R_c]^{2+\beta} [(t_0 - t_{0,c})\Gamma v/R_c + 1 - tv/R_c]}{[(t_0 - t_{0,c})/(t_{0,0} - t_{0,c})]^{\alpha_0}} dt_0 \quad (t_0 > t_{0,0}), \quad (28)$$

$$\tilde{t}_{0,\min} = \max\left\{t_{0,0}, \frac{t - R_c/v}{\Gamma} + t_{0,c}\right\} \quad (29)$$

and

$$\tilde{t}_{0,\max} = \frac{t - R_c/v + R_c/c}{(1 - v/c)\Gamma} + t_{0,c}, \quad (30)$$

where  $I_p$  is a constant and observation time  $t$  is confined by

$$(t_{0,0} - t_{0,c})(1 - v/c)\Gamma - R_c/c + R_c/v \leq t. \quad (31)$$

Not losing generality, we take  $t_{0,c} = 0$ . Equations (28)-(31) then become

$$h_p(t) = \int_{\tilde{t}_{0,\min}}^{\tilde{t}_{0,\max}} (1+t_0\Gamma v/R_c)^{2+\beta} (1+t_0\Gamma v/R_c - tv/R_c) (t_0/t_{0,0})^{-\alpha_0} dt_0 \quad (t_0 > t_{0,0}), \quad (32)$$

$$\tilde{t}_{0,\min} = \max\left\{t_{0,0}, \frac{t - R_c/v}{\Gamma}\right\}, \quad (33)$$

$$\tilde{t}_{0,\max} = \frac{t - R_c/v + R_c/c}{(1 - v/c)\Gamma} \quad (34)$$

and

$$(1 - v/c)\Gamma t_{0,0} - R_c/c + R_c/v \leq t. \quad (35)$$

Here, we take  $I_p\nu^{-\beta} = 1$  and  $\beta = 1$  to plot the light curves. For the Lorentz factor, we take  $\Gamma = 10$  and  $\Gamma = 100$ . We consider two typical values of the fireball radius  $R_c = 10^{15}cm$  and  $R_c = 10^{13}cm$ . For the intrinsic temporal power-law index, we take  $\alpha_0 = 2, 2.5, 3, 4$  and  $5$  respectively, and for the time when the power-law decay emission begins we take  $t_{0,0} = 0.01s, 0.1s$  and  $1s$  respectively.

The corresponding light curves are displayed in Fig. 3. Due to the contribution of  $h_p(t)$ , some new features are observed. There exist two kinds of light curve: a) a  $t^{-(2+\beta)}$  curve followed by a shallow decay curve with its index being obviously smaller than  $2 + \beta$  (type I); b) a  $t^{-(2+\beta)}$  curve followed by a very steep decay phase (shown as a “cutoff” curve) and then a shallow decay curve with its index being smaller than  $2 + \beta$  (type II). The curve of type II tends to appear in cases when the intrinsic temporal power-law index is large, the Lorentz factor is small and the onset of the intrinsic temporal power-law is early (comparing left panels of sub-figures a, b and c; or comparing right panels of the sub-figures). The very steep decay curve appears very close to the time position marked by that in the light curve arising from the  $\delta$  function emission (see the gray color lines in the figure) (in fact, relative to the latter, the former shifts to slightly larger time scales). This means that the time position of the very steep decay phase of the light curve of type II is mainly determined by the radius of the fireball, which can serve as an indicator of the latter (see also the discussion in the two previous subsections). For the light curve of type I, the start of the shallow decay phase can appear from very early time scale to around 300s for the fireball with radius  $R_c = 10^{13}cm$ , depending on the intrinsic temporal power-law index  $\alpha_0$ , the Lorentz factor  $\Gamma$  and the onset time  $t_{0,0}$  of the intrinsic temporal power-law (see the left panels of the sub-figures a, b and c). The smaller values of  $\alpha_0$ ,  $\Gamma$  and  $t_{0,0}$ , the larger time scale of the start of the shallow decay phase. For the fireball with radius  $R_c = 10^{15}cm$ , conclusions drawn from type I light curves remain the same, except that the maximum of the start time of the shallow decay phase can appear at around 3000s. In both types I and II, the slope of the shallow decay curve increases with the increasing of  $\alpha_0$ .

Revealed in the left lower panel of Fig. 3c, as a special case of type I, some light curves appear to be a single power-law one with their indexes significantly smaller than  $2 + \beta$ . They are in fact the shallow decay phase of the corresponding light curves. The onset of the phase shifts to much smaller time scales due to the larger values of the Lorentz factor  $\Gamma$  and the onset time  $t_{0,0}$  of the intrinsic temporal power-law for a given value of the fireball radius.

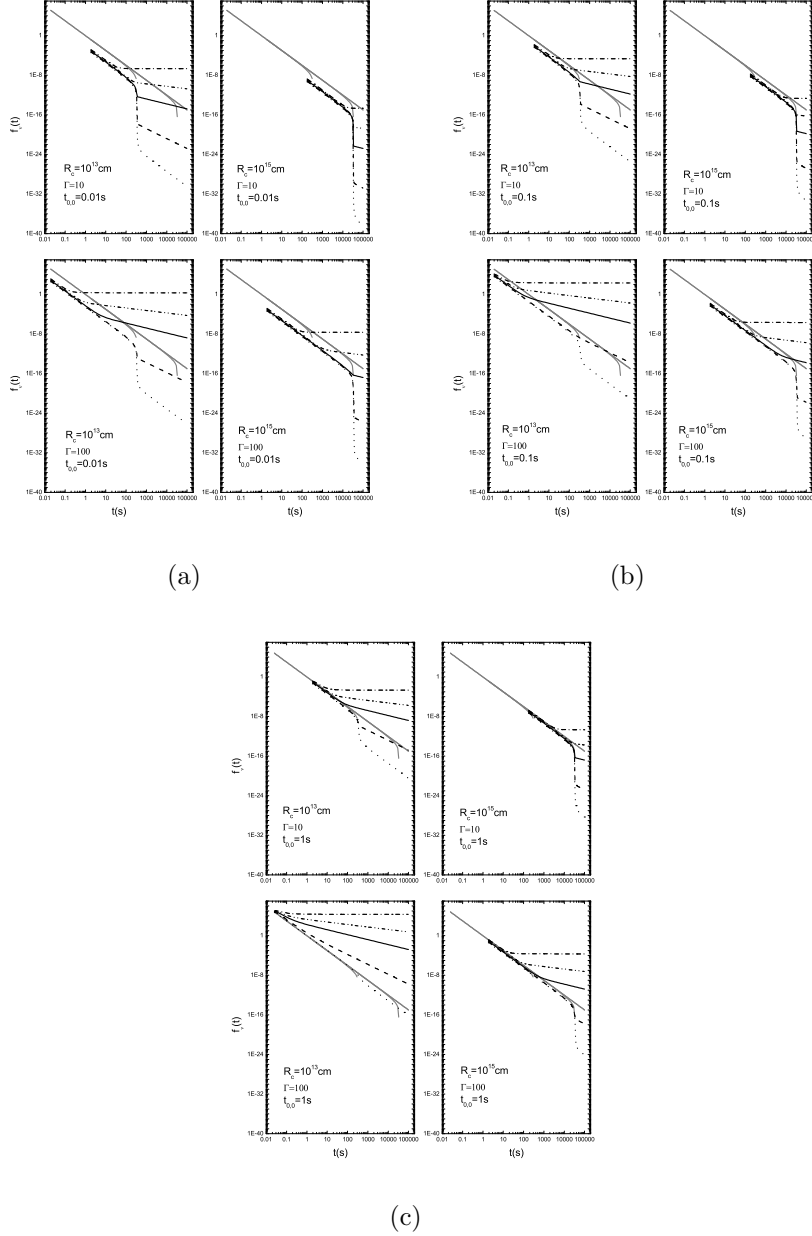


Fig. 3.— Light curves arising from the intrinsic emission with its temporal profile being a power-law function of time and the power-law decay time being infinity (see equation (27)), plotted in cases of  $t_{0,0} = 0.01s$  (sub-figure a),  $0.1s$  (sub-figure b) and  $1s$  (sub-figure c) respectively, where  $h_p(t)$  is determined by (32). The upper and lower panels of each sub-figure correspond to  $\Gamma = 10$  and  $\Gamma = 100$  respectively and the left and right panels of each sub-figure correspond to  $R_c = 10^{13}cm$  and  $R_c = 10^{15}cm$  respectively. Five kinds of black line stand for five different intrinsic temporal power-law indexes. They are (counting the five black lines for each panel from the top to the bottom): the dash dot line for  $\alpha_0 = 2$  ( $\alpha_0 = 1 + \beta$ ), the dash dot dot line for  $\alpha_0 = 2.5$  ( $\alpha_0 = 1.5 + \beta$ ), the solid line for  $\alpha_0 = 3$  ( $\alpha_0 = 2 + \beta$ ), the dash line for  $\alpha_0 = 4$  ( $\alpha_0 = 3 + \beta$ ) and the dot line for  $\alpha_0 = 5$  ( $\alpha_0 = 4 + \beta$ ). For the sake of comparison, those lines in Fig. 1 are also plotted (the grey color lines).

3.3.2. *When the power-law decay time is limited*

One might notice that there is no upper limit of the intrinsic power-law decay emission considered above. Let us put an upper limit to the intrinsic emission and then check if it could give rise to other noticeable features on the observed light curves. The intrinsic decaying light curve is assumed to be  $I_0(t_0) = [(t_0 - t_{0,c})/(t_{0,0} - t_{0,c})]^{-\alpha_0}$  for  $t_{0,0} < t_0 < t_{0,\max}$ . Also, we take  $t_{0,c} = 0$ . In this situation, equations (27), (32) and (33) hold, while equations (34) and (35) are replaced by

$$\tilde{t}_{0,\max} = \min\left\{t_{0,\max}, \frac{t - R_c/v + R_c/c}{(1 - v/c)\Gamma}\right\}, \quad (36)$$

$$(1 - v/c)\Gamma t_{0,0} - R_c/c + R_c/v \leq t \leq t_{0,\max}\Gamma + R_c/v. \quad (37)$$

Parameters adopted in producing Fig. 3 are also adopted here to create the light curves. Among those studied in Fig. 3, we consider only the following four cases:  $\Gamma = 10$  and  $t_{0,0} = 0.01s$  (see the upper panels of Fig. 3a);  $\Gamma = 10$  and  $t_{0,0} = 0.1s$  (see the upper panels of Fig. 3b);  $\Gamma = 100$  and  $t_{0,0} = 0.1s$  (see the lower panels of Fig. 3b);  $\Gamma = 100$  and  $t_{0,0} = 1s$  (see the lower panels of Fig. 3c). For the new parameter, we take  $t_{0,\max} = t_{0,0} + 0.01R_c/c$ ,  $t_{0,\max} = t_{0,0} + R_c/c$  and  $t_{0,\max} = t_{0,0} + 100R_c/c$  respectively. The corresponding light curves are displayed in Figs. 4-7 which correspond to the four cases respectively.

Upper panels of these figures show that when the power-law emission is as short as 0.01 times of the typical time scale of the fireball radius (say, when  $\Delta t_{0,0} = 0.01R_c/c$ ) and the Lorentz factor is not so large (say, not larger than 100), the light curves are similar to those arising from the  $\delta$  function emission. This suggests that, in the framework of the curvature effect, light curve characteristics of emissions with time scales as short as 0.01 times of  $R_c/c$  and the Lorentz factor not larger than 100 are hard to be distinguished from that of a  $\delta$  function emission. (This is in agreement with what is shown in Fig. 2.)

Lower panels of these figures arise from longer duration of the power-law emission ( $\Delta t_{0,0} = 100R_c/c$ ). Some new features appear. A remarkable one is the light curve with a power-law decay curve followed by a shallow phase and then a steeper power-law phase (type III). Connecting the two latter phases of this kind of light curve is a remarkable time break (check the upper three black lines of each lower panel of the figures). This tends to happen when the intrinsic temporal power-law index is relatively small. Otherwise, this kind of curve disappear (check the two lower black lines in each lower panel of the figures).

When the duration of the power-law emission is not so large and not so small (say,  $\Delta t_{0,0} = R_c/c$ ), other forms of light curves are observed (see the mid panels of these figures). In this situation, when the Lorentz factor is large enough (say,  $\Gamma = 100$ ), light curves of

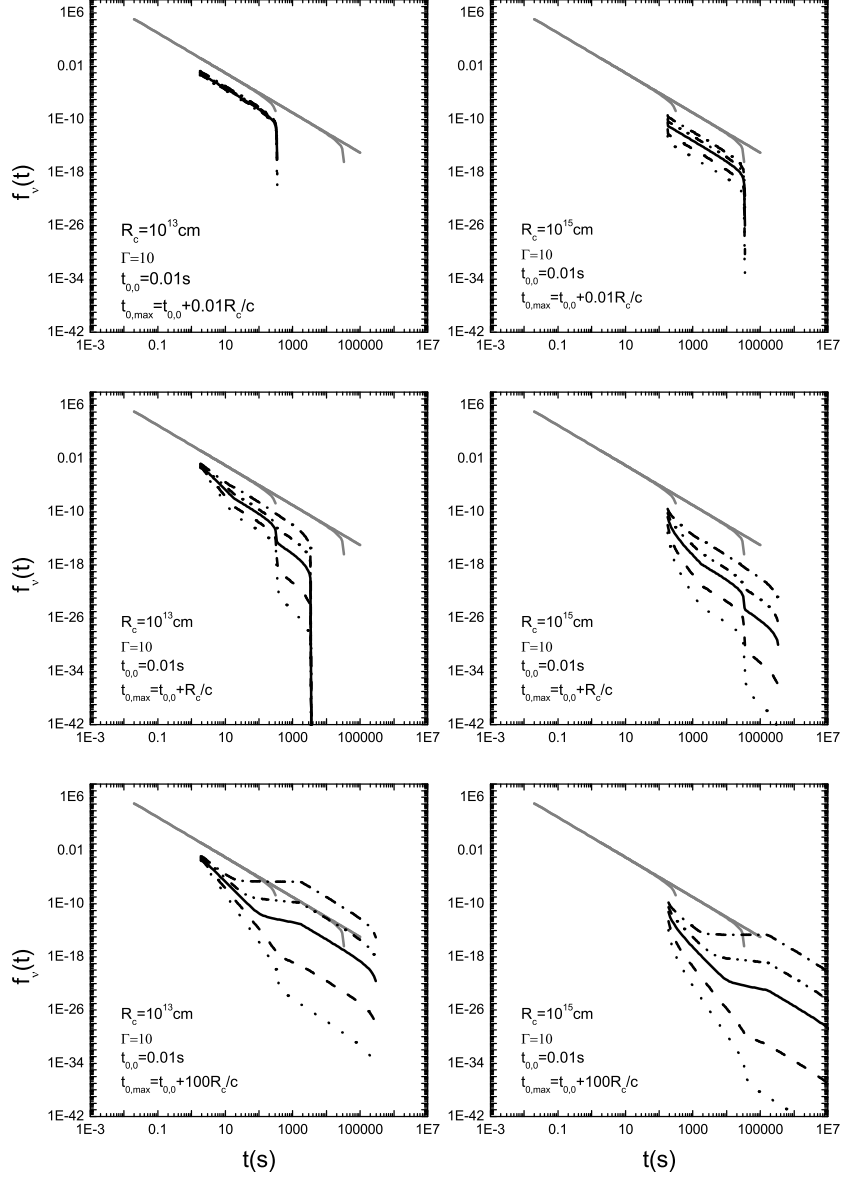


Fig. 4.— Light curves arising from the intrinsic emission with its temporal profile being a power-law function of time and with a limited duration, plotted in the case of  $\Gamma = 10$  and  $t_{0,0} = 0.01$  s. Here, we consider two values of the fireball radius and three time scales of the duration of the power-law emission (see the description in each panel). The equations are the same as that adopted in Fig. 3, except that we use equations (36) and (37) to replace equations (34) and (35), respectively. The symbols are the same as that in Fig. 3.

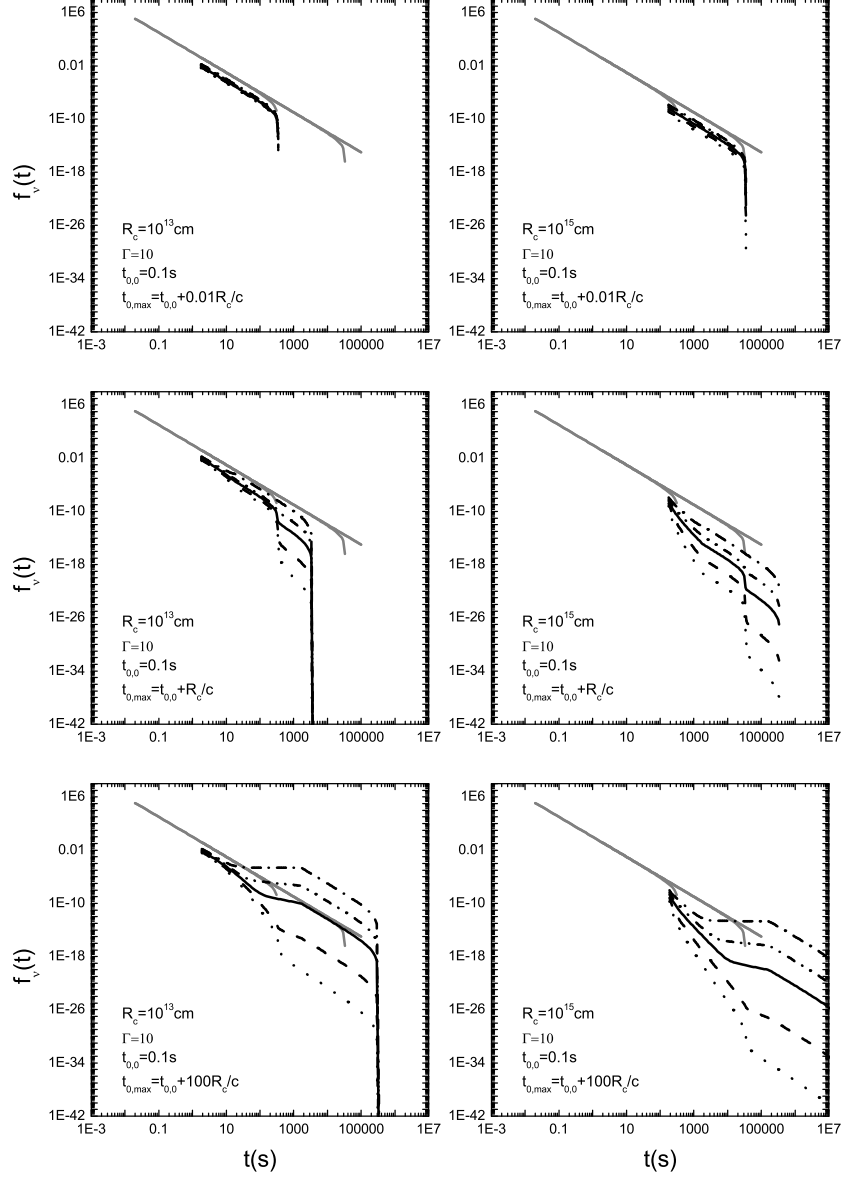


Fig. 5.— Light curves of Fig. 4 replaced by those produced in the case of  $\Gamma = 10$  and  $t_{0,0} = 0.1$  s.



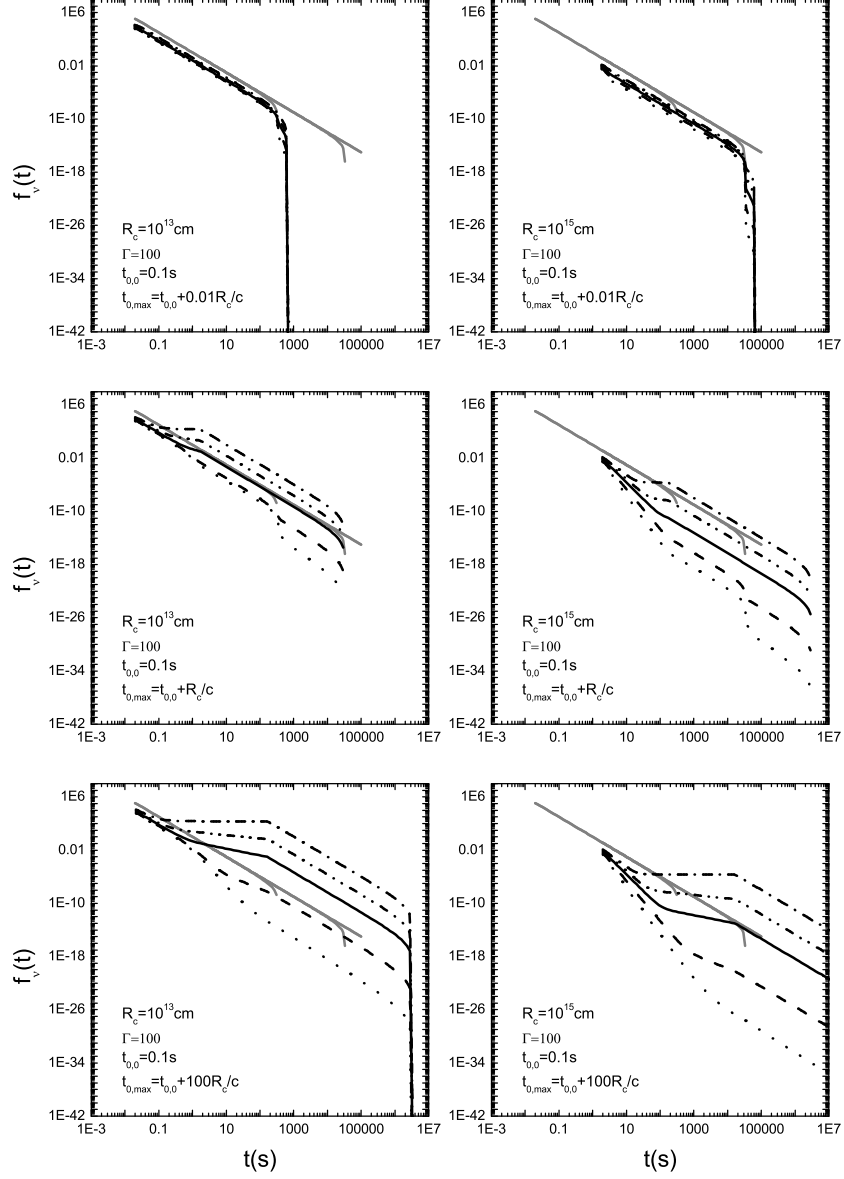


Fig. 6.— Light curves of Fig. 4 replaced by those produced in the case of  $\Gamma = 100$  and  $t_{0,0} = 0.1$  s.

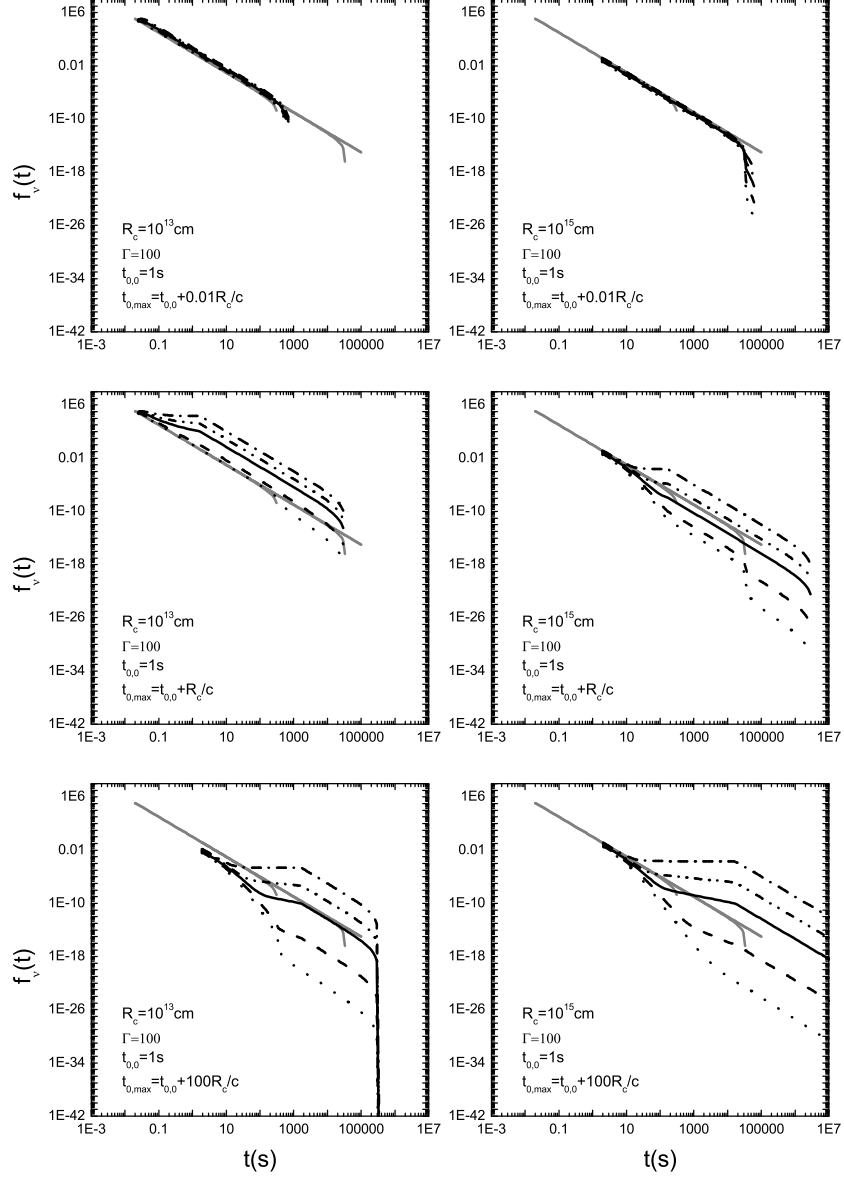


Fig. 7.— Light curves of Fig. 4 replaced by those produced in the case of  $\Gamma = 100$  and  $t_{0,0} = 1$  s.

type III with shorter shallow phases appear (see the mid panels of Figs. 6 and 7). This is expectable since in the framework of the curvature effect the profile of a light curve depends only on the ratio between the observational time scale and the corresponding fireball radius time scale  $R_c/c$  (see Qin et al. 2004), and due to the contraction time effect (note that, the face-on part of the fireball surface moves towards us when the fireball expands) a certain observational time scale corresponds to a longer co-moving time scale for a larger Lorentz factor.

#### 4. Example of application

In our analysis above, we consider only a simple power-law emission, for which the power-law index  $\beta$  is assumed to be constant. Expected from the model, the observed spectrum would be a constant power-law with the same index and the rapid decay light curve would be the well-known  $t^{-(2+\beta)}$  curve. This constrains our application, since the spectra of many X-ray afterglows of GRBs are found to vary with time and the corresponding light curves are found not to follow the  $t^{-(2+\beta)}$  curve (see Zhang et al. 2007 and the UNLV GRB Group web-site <http://grb.physics.unlv.edu>). Instead of a power-law, many light curves are bent. To apply our model, one must find a burst with its spectral index being constant and its light curve following (or approximately following) the  $t^{-(2+\beta)}$  curve in its X-ray afterglow.

After checking the data provided in web-site <http://grb.physics.unlv.edu> (up to March 25, 2008), we find that GRB 050219A might be one that fits our simple model. The data show, the spectral index does not vary with time and its mean is  $\beta = 0.907 \pm 0.051$ . In addition, the first decay curve of the burst is a power-law curve with its index being approximately  $2+\beta$ . This phase is followed by a shallow one which starts at about 500s. Comparing this light curve with those presented in Fig. 3, we guess, if it is due to the curvature effect, the fireball radius must be larger than  $R_c = 10^{13}cm$ , otherwise the start time of the shallow phase would be too small to meet the data (see the left panels of Figs. 3a, 3b and 3c). If the radius is  $R_c = 10^{15}cm$ , then the Lorentz factor must be larger than 10, otherwise the start time of the shallow phase would be too large (see the right upper panels of Figs. 3a, 3b and 3c). Revealed in Fig. 3, there are four factors affecting the start time of the shallow phase: the fireball radius  $R_c$ ; the Lorentz factor  $\Gamma$ ; the intrinsic temporal power-law emission index  $\alpha_0$ ; and the start time of the intrinsic temporal power-law emission  $t_{0,0}$ .

Available in the mentioned web-site, there are 75 data points in the XRT light curve of GRB 050219A. As an example of fitting, we ignore the three data points with the largest time scales since the gap between them and the majority of the data set is too large and the domain showing a constant spectral index does not cover them (see <http://grb.physics.unlv.edu>) (in

this way, one cannot tell if the spectral index in the corresponding time scale is still constant). With the rest 72 data points, we need only apply the equations adopted in the discussion of the case of the temporal profile of the intrinsic emission being a power-law function of time and the power-law decay time being infinity. The equations adopted in producing Fig. 3 are employed to fit the data set, where the term  $I_p\nu^{-\beta}$ , which dominates the magnitude of the theoretical curve, would be determined by fit.

Since both the fireball radius and the Lorentz factor are sensitive to the time scale of the start time of the shallow phase, we deal with them one by one. We first fix the Lorentz factor and assume it to be  $\Gamma = 100$ , allowing  $R_c$  and  $\alpha_0$  to vary since not only the start time of the shallow phase should be met but also the power-law index of the shallow phase should be accounted for. In addition, we take  $t_{0,0} = 1s$  since  $t_{0,0}$  is less sensitive to the start time of the shallow phase (see the right panels of Figs. 3a, 3b and 3c). The best fitting curve is shown in Fig. 8. One finds that the XRT data of GRB 050219A can be roughly accounted for by a power-law temporal emission from an expanding fireball surface. Note that the corresponding fitting parameters are not important since other possibilities exist (see the discussion below).

Next, we fix the fireball radius and take it as  $R_c = 10^{15}cm$  (in fact, we take  $R_c/v = (1/3)10^5s$  which corresponds to  $R_c \simeq 10^{15}cm$ ), allowing  $\Gamma$  and  $\alpha_0$  to vary. Also, we take  $t_{0,0} = 1s$ . The best fit is displayed in Fig. 9. It shows that the result of the fit with a fixed fireball radius is hard to be distinguished from that with a fixed Lorentz factor. Therefore, the resulting fitting parameters are not important in this stage of investigation.

There is a third choice: one could fix  $\alpha_0$  and allow  $R_c$  and  $\Gamma$  to vary. We guess, it might yields a similar result.

## 5. Discussion and conclusions

We investigate in this paper how an intrinsic emission with a power-law spectrum  $I_{0,\nu}(t_0, \nu_0) = I_0(t_0)\nu_0^{-\beta}$  emitting from an expanding fireball surface gives rise to an observed flux density when the full curvature effect is considered. We find that, if the power-law spectrum of the intrinsic radiation holds within the energy range that corresponds to the observed energy channel due to the Doppler shifting, the resulting spectrum would be a power-law as well and the index will be exactly the same as that in the intrinsic spectrum, regardless the real form of the temporal profile of the intrinsic emission. Accompanied with the power law spectrum of index  $\beta$  is a power law light curve with index  $2 + \beta$ , expected by the curvature effect, which was known previously (see Fenimore et al. 1996; Kumar &

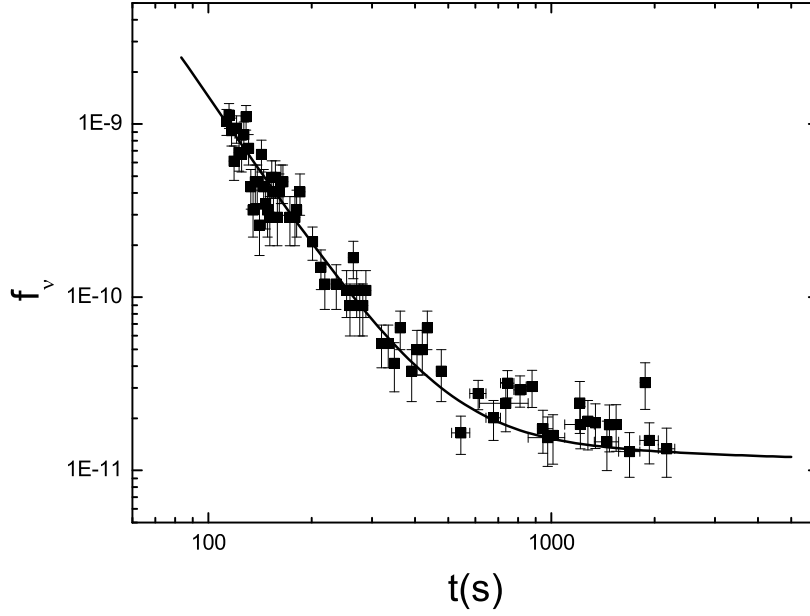


Fig. 8.— XRT light curve of GRB 050219A. Equations (27) and (32)-(35), which describe light curves arising from the intrinsic emission with its temporal profile being a power-law function of time and the power-law decay time being infinity, are employed to fit the data, where we take  $\Gamma = 100$ . The solid line is the best fit to the data. The corresponding fitting parameters are:  $R_c = 1.05 \times 10^{16} cm$ ,  $\alpha_0 = 2.05$ , and  $I_p \nu^{-\beta} = 9.56 \times 10^{-4}$  (see equation (27)). The  $\chi^2$  of the fit is  $\chi_{dof}^2 = 1.39$ .

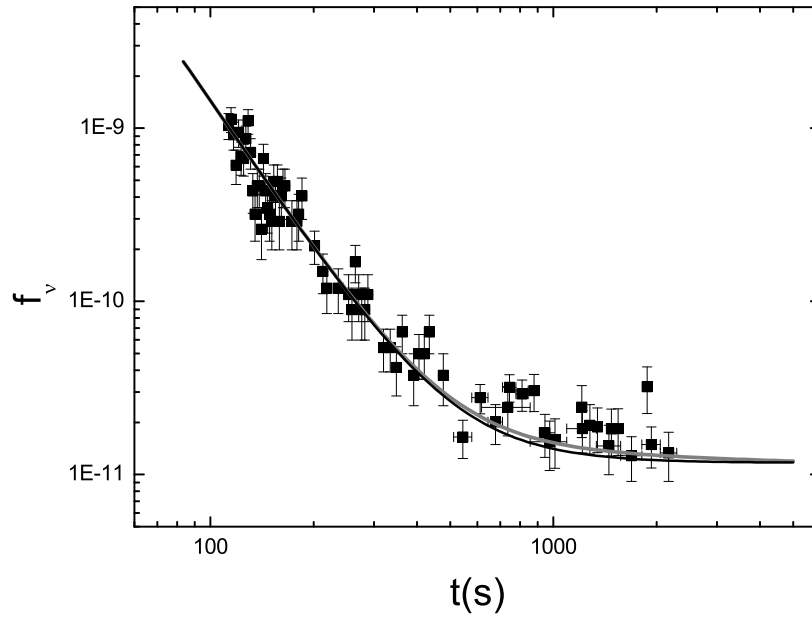


Fig. 9.— Another fit to the XRT light curve of GRB 050219A, where we take  $R_c/v = (1/3)10^5 s$ . The equations adopted for the fit are the same as those used in Fig. 8. The black solid line represents the best fit and the grey solid line is the solid line in Fig. 8. The corresponding fitting parameters are:  $\Gamma = 23.1$ ,  $\alpha_0 = 1.98$ , and  $I_p \nu^{-\beta} = 8.88 \times 10^{-4}$  (see equation (27)). The  $\chi^2$  of the fit is  $\chi_{dof}^2 = 1.48$ .

Panaitescu 2000). This light curve could be observed if the intrinsic emission is extremely short or if the emission arises from an exponential cooling.

In particular, we assume and consider a power-law cooling emission in the co-moving frame (for this emission, the intrinsic temporal profile is a power-law). We find that, if the power-law decay time being infinity, due to the contribution of the power-law cooling in the co-moving frame, the observed light curve influenced by the full curvature effect contains two phases: one is a rapid decay phase where the light curve well follows the well-known  $t^{-(2+\beta)}$  curve, and the other is a shallow decay phase where the light curve is obviously shallower than that in the rapid decay phase. If the power-law decay time is limited, there would be several kinds of light curve. A remarkable one among them contains three power-law phases (see Figs. 4-7): the first is a rapid one with its index being equal to or larger than that of the  $t^{-(2+\beta)}$  curve; the second is a shallow decay one with its index being obviously smaller than that in the first phase; and the third is a rapid decay one with its index being equal to or less than that of the first phase. It might be possible that, some of the GRBs containing such features in their afterglow light curves are due to expanding fireballs or face-on uniform jets (see e.g. Qin et al. 2004) emitting with a power-law spectrum and a power-law cooling (being infinity or limited). In the view of co-moving observers, the dynamic process of the merger of shells would be somewhat similar to that occurred in the external shocks (the main difference is that in the case of inner shocks, a co-moving observer observes only a limited volume of medium for which the density would evolve with time due to the enhancement of the fireball surface). Based on this argument, we suspect that the intrinsic emission of some of those bursts possessing in their early X-ray afterglows a rapid decay phase soon followed by a shallow decay phase and then a rapid decay one might be somewhat similar to the well-known standard forward shock model (Sari et al. 1998; Granot et al. 1999); while for some of the bursts with a rapid phase followed by a shallow phase in their late X-ray afterglows the emission might be that of the standard forward shock model influenced by the curvature effect. Necessary conditions for perceiving this mechanism include: a) during the period concerned, the spectral index should be constant; b) the temporal index in the first phase should be equal to or larger than that of the  $t^{-(2+\beta)}$  curve.

As an example of application, we employ the XRT data of GRB 050219A to perform a fit since the spectral index  $\beta$  of this burst does not vary with time and the first decay phase of its light curve is a power-law one with its index being approximately  $2 + \beta$ . The result shows that the XRT data of this burst can be roughly accounted for by a power-law temporal emission from an expanding fireball surface. Since there exist various possibilities, parameters obtained by the fit are not unique. To determine the parameters, we need other independent estimations. According to the analysis above, a reliable value of the fireball radius would be obtained if one observes a “cut-off” feature following the  $t^{-(2+\beta)}$  curve in

the case of a constant spectral index  $\beta$ . Nevertheless, the start time of the shallow phase could raise a limit to the fireball radius (see Figs. 3-7). For GRB 050219A, if its XRT data are indeed due to the curvature effect, its radius corresponding to this emission must be larger than  $R_c = 10^{13}cm$ . We have checked that taking  $R_c/v = (1/3)10^4s$  (which corresponds to  $R_c \simeq 10^{14}cm$ ),  $\Gamma = 8$  and  $\alpha_0 = 2.157$  can also roughly account for the data. As the Lorentz factor is so small in this situation, we conclude that, if the X-ray afterglow of GRB 050219A does arise from the emission of an expanding fireball surface, the radius of the fireball associated with this emission would not be much less than  $R_c = 10^{14}cm$ , otherwise  $\Gamma$  would be too small to be regarded as a relativistic motion.

Why a shallow phase emerges due to the curvature effect? We guess, while the first phase is dominated by the geometric effect and therefore obeys the  $t^{-(2+\beta)}$  curve, in the shallow phase the intrinsic emission overcomes the geometric effect and dominates the light curve observed. One might notice the  $\alpha_0 = 2$  lines (the dash dot lines) in Fig. 3 — the shallow phase curve of these lines is parallel to the time axis. As the radius grows linearly with time when a constant Lorentz factor is assumed (see Qin 2002), the emission from the fireball surface of a certain solid angle increases as a square of time (the area of the surface is proportional to  $R^2$ ). This in turn makes the total emission of  $I_0 \propto t_0^{-2}$  from the surface becoming constant. When the intrinsic emission overcomes the geometric effect in the shallow phase, one cannot expect a light curve of  $t^{-\alpha_0}$ , but instead, we expect that of  $t^{-(\alpha_0-2)}$  (see Fig. 3).

It is known that a  $\delta$ -function intensity approximates the process of an extremely short emission. This will occur when the corresponding fireball shells are very thin and the cooling time is relatively short compared with the curvature time scale (for the time scale of the curvature effect, see Kocevski et al. 2003 and Qin & Lu 2005). Two light curve characteristics are associated with a quasi- $\delta$ -function emission. The first is a strict power-law decay curve with index  $2 + \beta$ . The second is the limited time range of this curve. If the cooling time is not so short but it is an exponential one, then these characteristics are also expected (see Fig. 2). Note that the exponential cooling time does not last the  $t^{-(2+\beta)}$  curve to a much larger time scale when the cooling itself is not very large (say, in the case of  $R_c = 10^{15}cm$ ,  $\sigma_d < 100s$ ; see Fig. 2). Thus, one can estimate the fireball radius from bursts possessing these characteristics (note that, the time scale of the  $t^{-(2+\beta)}$  curve is independent of the Lorentz factor; see equations (16) and (18)). For candidates of this kind of burst, we propose to fit the spectrum with  $\nu^{-\beta}$  and the light curve with  $[T_D - (t - T_0)](t - T_0)^{-(2+\beta)}$ , where both  $T_D$  and  $T_0$  are free parameters. When the fitting is good enough, we say that the intrinsic fireball emission is likely very short or the cooling is an exponential one and the corresponding fireball radius is  $R_c \simeq vT_D$ . When the expansion of the fireball is relativistic, we get  $R_c \simeq cT_D$ . Therefore, via this method, one obtains at least the upper limit of the fireball radius as long



as the intrinsic emission is extremely short, or the cooling is an exponential one, and the intrinsic spectrum is a power-law.

In the case of the intrinsic temporal power-law emission, when its temporal index is large enough ( $\alpha_0 > 2 + \beta$ ), there would be a “cutoff” curve located exactly at the same time position of the speedily falling off tail in the light curve of a  $\delta$ -function emission. This feature could be used to estimate the fireball radius as well. Presented in Zhang et al. (2007), several bursts seem to possess this “cutoff” feature: GRB050724, GRB060211A, GRB060218, GRB060427, GRB060614, GRB060729 and GRB060814. If the proposed interpretation can be applied, their radius would be that ranging from  $10^{13}cm$  to  $10^{15}cm$ . At least one reason prevents us to reach such a conclusion. The spectra of these bursts happen to vary quite significantly within the light curves associated with this feature. This conflicts with what we assume in this paper (we assume a constant intrinsic spectrum). We thus appeal further investigation of this issue taking into account the variation of the intrinsic spectrum, which might tell us whether the “cutoff” feature remains and/or its properties are maintained.

Displayed in literature, many Swift bursts are found to possess a bent light curve instead of a strict power-law one, in the early X-ray afterglow (see, e.g., Chincarini et al. 2005; Liang et al. 2006; Nousek et al. 2006; O’Brien et al. 2006). In our analysis above, we seldom get bent light curves. This must be due to the fact that the model concerned is too simple, where we consider only emissions with constant spectra. When the intrinsic spectrum varies with time, one would expect bursts with both variable spectra and bent light curves (the well-known  $t^{-(2+\beta)}$  curve suggests that light curves of fireballs are strongly affected by the corresponding emission spectra). Indeed, we find that both variable spectra and bent light curves happen to appear in the same period for many Swift bursts (see Zhang et al. 2007 and the UNLV GRB Group web-site <http://grb.physics.unlv.edu>).

Since for some bursts their early X-ray afterglow spectra evolve with time while for some others their spectra have no significant temporal evolution (Zhang et al. 2007; Butler & Kocevski 2007b), we suspect that there might be two kinds of mechanism accounting for the X-ray afterglow emission. It seems likely that the observed variation of spectra is due to an intrinsic spectral evolution. The intrinsic spectral evolution would probably lead to deviations of the light curves studied above (those studied in Figs. 3-7). We thus suspect that the bursts with no spectral evolution might have “normal” temporal profiles, while others might exhibit somewhat “abnormal” profiles. This seems to be the case according to Figs. 1-3 in Zhang et al. (2007) and Figs. 7-8 in Butler & Kocevski (2007b).

Our simple model tends to account for the kind of bursts that their X-ray afterglow spectra do not evolved with time. However, for many bursts with roughly constant spectra and power-law light curves, the curves are too shallow to be accounted for by the  $t^{-(2+\beta)}$

curve (see <http://grb.physics.unlv.edu>). Our model seems too simple to account for the majority of XRT light curve data of Swift bursts. It is therefore necessary to explore more complicated cases. For example, a variant Lorentz factor (which is expectable when the intrinsic emission is long enough) might play a role. Would it affect the slope of the decaying curve? We are looking forward to see more investigations on this issue in the near future.

Before ending this paper, we would like to point out that quantity  $t_{0,c}$  is the co-moving time measured by a co-moving observer when the fireball radius reaches  $R_c$  (see Qin 2002). Note that,  $t_{0,0} > t_{0,c}$ . Therefore, when assigning  $t_{0,c} = 0$ ,  $t_{0,0} = 1s$  means 1s co-moving time has passed after  $R = R_c$ . When one analyzes the emission associated with  $R_c = 10^{15}cm$ ,  $t_{0,0} = 0$  refers only the emission at  $t_{0,c} = 0$  which is the co-moving time when  $R = R_c$ . Although we take quite small values of  $t_{0,0}$  in the above analysis, it does not correspond to early emission when we adopt  $R_c = 10^{15}cm$  or  $R_c = 10^{13}cm$ . Therefore, our analysis on emission from fireballs with  $R_c = 10^{15}cm$  does not put forward any constraint on the prompt emission. The conclusion that characteristics of the prompt emission of bursts with shallow decay phase are similar to those without shallow decay phase obtained recently by Liang et al. (2007) are not violated by our findings.

This work was supported by the National Science Fund for Distinguished Young Scholars (10125313), the National Natural Science Foundation of China (No. 10573005), and the Fund for Top Scholars of Guangdong Province (Q02114). We also thank the financial support from the Guangzhou Education Bureau and Guangzhou Science and Technology Bureau.

## REFERENCES

- Barthelmy, S. D. et al. 2005, ApJ, 635, L133
- Butler, N. R. & Kocevski, D. 2007a, ApJ, 663, 407
- Butler, N. R. & Kocevski, D. 2007b, ApJ, accepted, (astro-ph/0702638)
- Chincarini, G. et al. 2005, preprint, (astro-ph/0506453)
- Cusumano, G. et al. 2006, ApJ, 639, 316
- Dermer, C. D. 2004, ApJ, 614, 284
- Dyks, J. et al. 2005, preprint, astro-ph/0511699
- Fenimore, E. E. et al. 1996, ApJ, 473, 998

- Granot, J., Piran, T., Sari, R. 1999, ApJ, 513, 679
- Kocevski, D., Ryde, F., Liang, E. 2003, ApJ, 596, 389
- Kumar, P. & Panaitescu, A. 2000, ApJ, 541, L51
- Liang, E. W. et al. 2006, ApJ, 646, 351
- Liang, E. W. et al. 2007, ApJ, 670, 565 (astro-ph/0705.1373)
- Lu, R.-J., Qin, Y.-P., Zhang, Z.-B., Yi, T.-F. 2006, MNRAS, 367, 275
- Nousek, J. A. et al. 2006, ApJ, 642, 389
- O'Brien, P. T. et al. 2006, ApJ, 647, 1213
- Panaitescu, A. et al. 2006, MNRAS, 366, 1357
- Peng, Z.-Y., Qin, Y.-P., Zhang, B.-B., Lu, R.-J., Jia, L.-W., Zhang, Z.-B. 2006, MNRAS, 368, 1351
- Qin, Y.-P. 2002, A&A, 396, 705
- Qin, Y.-P. et al. 2004, ApJ, 617, 439
- Qin, Y.-P. & Lu, R.-J. 2005, MNRAS, 362, 1085
- Qin, Y.-P. et al. 2005, ApJ, 632, 1008
- Qin, Y.-P. et al. 2006, Phys. Rev. D 74, 063005
- Ryde, F. & Petrosian, V. 2002, ApJ, 578, 290
- Sari, R., & Piran, T. 1997, ApJ, 485, 270
- Sari, R., Piran, T., & Narayan, R. 1998, ApJ, 497, L17
- Shen, R.-F. et al. 2005, MNRAS, 362, 59
- Tagliaferri, G. et al. 2005, Nature, 436, 985
- Vaughan, S. et al. 2006, ApJ, 638, 920
- Zhang, B., Fan, Y. Z., Dyks, J. et al. 2006, ApJ, 642, 354
- Zhang, B.-B. et al. 2007, ApJ, in press, (astro-ph/0612246)

Zhang, B. 2007, ChJAA, 7, 1